Targeting Cell Surface Receptors with Ligand-Conjugated Nanocrystals

ARTICLE *in* JOURNAL OF THE AMERICAN CHEMICAL SOCIETY · JUNE 2002

Impact Factor: 12.11 · DOI: 10.1021/Ja003486s · Source: PubMed

J|A|C|S
ARTICLES
Published on Web 04/05/2002

Targeting Cell Surface Receptors with Ligand-Conjugated Nanocrystals

Sandra J. Rosenthal,*,† Ian Tomlinson,† Erika M. Adkins,‡ Sally Schroeter,‡ Scott Adams,‡ Laura Swafford,† James McBride,† Yongqiang Wang,† Louis J. DeFelice,‡ and Randy D. Blakely‡

Contribution from the Department of Chemistry, and the Department of Pharmacology, Vanderbilt University School of Medicine, Vanderbilt University, Nashville, Tennessee 37235

Received September 25, 2000. Revised Manuscript Received September 10, 2001

Abstract: To explore the potential for use of ligand-conjugated nanocrystals to target cell surface receptors, ion channels, and transporters, we explored the ability of serotonin-labeled CdSe nanocrystals (SNACs) to interact with antidepressant-sensitive, human and *Drosophila* serotonin transporters (hSERT, dSERT) expressed in HeLa and HEK-293 cells. Unlike unconjugated nanocrystals, SNACs were found to dose-dependently inhibit transport of radiolabeled serotonin by hSERT and dSERT, with an estimated half-maximal activity (EC_{50}) of 33 (dSERT) and 99 μM (hSERT). When serotonin was conjugated to the nanocrystal through a linker arm (LSNACs), the EC_{50} for hSERT was determined to be 115 μM. Electrophysiology measurements indicated that LSNACs did not elicit currents from the serotonin-3 ($5HT_3$) receptor but did produce currents when exposed to the transporter, which are similar to those elicited by antagonists. Moreover, fluorescent LSNACs were found to label SERT-transfected cells but did not label either nontransfected cells or transfected cells coincubated with the high-affinity SERT antagonist paroxetine. These findings support further consideration of ligand-conjugated nanocrystals as versatile probes of membrane proteins in living cells.

Introduction

Semiconductor nanocrystals such as those consisting of CdSe (Figure 1) have received substantial attention due to their size-tunable optical properties.[1] Nanocrystals, or "quantum dots", have the same crystal structure as the bulk material but consist of only a few hundred to a few thousand atoms. Due to incomplete surface passivation resulting in dangling bonds at the nanocrystal surface, nanocrystals have a low fluorescent quantum yield. However, when a "core" nanocrystal is passivated in a "shell" of a wider bandgap semiconductor material, the resulting nanocrystal becomes highly luminescent.[2−4] Core/shell nanocrystals have several advantages over organic molecules as fluorescent labels for biological applications, including resistance to photodegradation, improved brightness, and size-dependent, narrow-emission spectra that enable the monitoring of several processes simultaneously.[5,6] Additionally, their absorption spectrum is continuous above the band gap so that any standard, inexpensive, excitation source can be used to excite the nanocrystal. To target fluorescent nanocrystals to biological molecules, core/shell nanocrystals must be derivatized. Recently, two reports demonstrated the use of ligand-conjugated, fluorescent nanocrystals as biological labels.[5,6] In a two-color experiment using mouse fibroblasts, Bruchez et al.[5] used small, green fluorescent core/shells coated with methoxysilylpropylurea and acetate groups to stain the cell nucleus and larger, red fluorescent core/shells coated with biotin to label F-actin filaments preincubated with phalloidin−biotin and streptavidin. In a second experiment, Chan and Nie[6] linked the protein transferrin to the surface of core/shells and found the nanocrystal−transferrin conjugates were internalized by HeLa cells through receptor-mediated endocytosis. In a slightly different application, Chunyang et al.[7] conjuagated the protein trichosanthin to the surface of core/shell nanocyrstals and found that the enzymatic activity of the protein was not inhibited when conjugated to the quantum dot. Furthermore, these nanoconjugates were found to aggregate in the cytoplasm of human choriocarinoma cells.[7]

One specific use of ligand-conjugated nanocrystals that has not been explored is the targeting of these probes to cell surface receptors, ion channels, and transporters via specific organic ligands or drugs. Chemical signaling in the nervous system involves the coordinated action of a large number of these cell surface proteins. Among these proteins are the neurotransmitter

† Department of Chemistry.
‡ Department of Pharmacology, Vanderbilt University School of Medicine.

(1) For a review of the size-dependent properties of semiconductor nanocrystals, see: Alivisatos, A. P. *J. Phys. Chem.* **1996**, *100*, 13226−13239.
(2) Hines, M. A.; Guyot-Sionnest, P. *J. Phys. Chem.* **1996**, *100*, 468−471.
(3) Dabbousi, B. O.; Rodriguez-Viejo, Mikulec, F. V.; Heine, J. R.; Mattoussi, H.; Ober, R.; Jensen K. F.; Bawendi M. G. *J. Phys. Chem. B* **1997**, *101*, 9463−9475.
(4) Peng, X.; Schlamp, M. C.; Kadananich, A. V.; Alivisatos, A. P. *J. Am. Chem. Soc.* **1997**, *119*, 7019−7029.
(5) Bruchez, M., Jr.; Moronne, M.; Gin, P.; Weiss, S.; Alivisatos, A. P. *Science* **1998**, *281*, 2013−2016.
(6) Chan, W. C. W.; Nie, S. *Science* **1998**, *281*, 2016−2018
(7) Chunyang, Z.; Hui, M.; Nie, S.; Yao, D.; Lei, J.; Dieyan, C. *Analyst* **2000**, *125*, 1029−1031.

10.1021/ja003486s CCC: $22.00

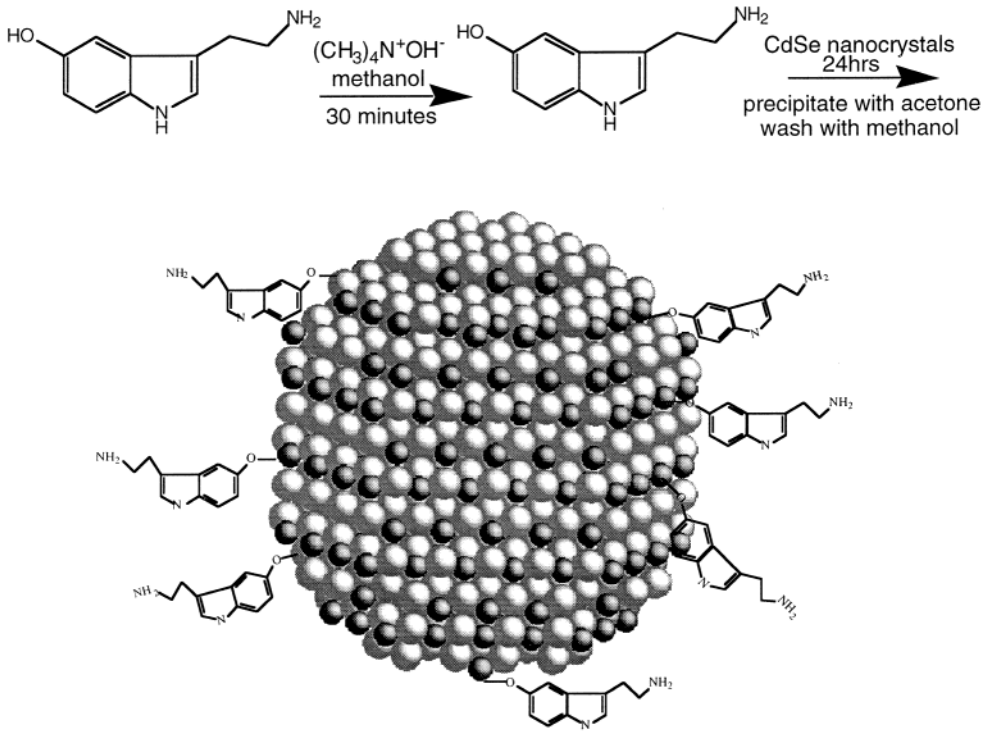

Figure 1. The neurotransmitter serotonin (5-hydroxytryptamine, 5-HT) and the preparation of serotonin-labeled nanocrystals (SNACs).

transporters that are responsible for the termination of neurotransmitter signal by clearing these small molecules from extracellular spaces following release. More than a dozen related transporters provide for the clearance of different neurotransmitters, including serotonin (5-hydroxytryptamine, Figure 1), dopamine, norepinephrine, and GABA.[8,9] Drugs that selectively target the norepinephrine and serotonin transporters are in widespread clinical use as antidepressants.[10] The psychostimulants cocaine and amphetamines also compete for transmitter access with dopamine, norepinephrine, and serotonin transporters, and by blocking amine uptake or inducing efflux, they bring about elevated extracellular levels of these substances, inducing alterations in locomotor activity, appetite, and cognition. Although the importance of transporter proteins as drug targets has been known for decades, only recently has it become apparent that transporter-mediated clearance of neurotransmitters is under tight regulation, including the polarized expression of transporter proteins,[11,12] protein kinase-mediated alterations in cell surface expression,[13] and activity-dependent phosphorylation and redistribution.[14,15] These latter properties are similar to the dynamics associated with G protein-coupled receptors and ligand-gated ion channels which are also expressed nonuniformly on neurons and can be induced to relocalize in response to cell stimuli.[16−19] Advances in understanding basic mechanisms supporting patterns of transporter localization and regulation require tools sufficient to localize transporter proteins in situ in living cells. Currently, the detection, quantitation, and localization of membrane proteins is achieved largely by radiolabeled ligands or indirectly with antibody techniques.[20,21] These approaches are limited due to the poor spatial resolution of autoradiographic methods, the limited availability of surface domain-selective antibody probes for membrane proteins, and the broad emission spectra and photochemical degradation of available fluorophores. Ligand-conjugated fluorescent nanocrystals are potentially a solution to these difficulties.

In this paper, we demonstrate that serotonin-labeled nanocrystals (SNACs) interact with the serotonin transporter protein (SERT) in transfected HeLa cells and oocytes in vitro. We also demonstrate that fluorescent SNACs can be used to visualize SERTs expressed in human epithelial kidney (HEK) cells in an antidepressant-sensitive manner.

Experimental Section

SNACs. The 30-Å trioctylphosphine oxide-coated (TOPO) CdSe nanocrystals were prepared by the method of Murray et al.[22] as modified by Peng et al.[23] SNACs were prepared by first reacting 60 mg of serotonin and 1 mL of a 20% tetramethylammonium hydroxide/

(8) Miller, J. W.; Kleven, D. T.; Domin, B. A.; Freemeau, R. T., Jr. In *Neurotransmitter Transporters: Structure, Function and Regulation*; Reith, M. E. A., Ed.; Humana Press: Totowa, NJ, 1997.
(9) Povlock, S. L.; Amara, S. G. In *Neurotransmitter Transporters: Structure, Function and Regulation*; Reith, M. E. A., Ed.; Humana Press: Totowa, NJ, 1997.
(10) Barker, E. L.; Blakely, R, D. In *Psychopharmacology: The Fourth Generation of Progress*; Bloom, F. E., Kupfer, D. J., Eds.; Raven Press: New York, 1995.
(11) Schroeter, S.; Levey, A. I.; Blakely, R. D. *Mol. Cell. Neurosci.* **1997**, *9*, 170−184.
(12) Gu, H. H.; Ahn, J.; Caplan, M. J.; Blakely, R. D.; Levey, A. I.; Rudnick, G. *J. Biol. Chem.* **1996**, *271*, 18100−18106.
(13) Qian, Y.; Galli, A.; Ramamoorthy, S.; Risso, S.; DeFelice, L. J.; Blakely, R. D. *J. Neurosci.* **1997**, *17*, 45−57
(14) Ramamoorthy, S.; Giovanetti, E.; Qian, Y.; Blakely, R. D. *J. Biol. Chem.* **1998**, *273*, 2458−2466.
(15) Ramamoorthy, S.; Blakely, R. D. *Science* **1999**, *285*, 763−766.
(16) Mantyh, P. W.; Demaster, E.; Malhotra, A.; Ghilardi, J. R.; Rogers, S. D.; Mantyh, C. R.; Liu, H.; Basbaum, A. I.; Vigna, S. R.; Maggio, J. E.; Simone, D. A. *Science* **1995**, *268*, 1629−1632.
(17) Keith, D. E.; Murray, S. R.; Zaki, P. A.; Chu, P. C.; Lissin, D. V.; Kang, L.; Evans, C. J.; von Zastrow, M. *J. Biol. Chem.* **1996**, *271*, 19021−19024.
(18) Rao, A.; Craig A. M. *Neuron* **1997**, *19*, 801−812.
(19) Lissin, D. V.; Gomperts, S. N.; Carroll, R. C.; Christine, D. W.; Kalman, D.; Kitamura, M.; Hardy, S.; Nicoll, R. A.; Malenka, R. C.; von Zastrow, M. *Proc. Natl. Acad. Sci. U.S.A.* **1998**, *95*, 7097−7102.
(20) Qian, Y.; Melikian, H. E.; Rye, D. B.; Levey, A. I.; Blakely, R. D. *J. Neurosci.* **1995**, *15*, 1261−1274.
(21) Limbird, L. E. *Cell Surface Receptors: A Short Course on Theory and Methods*, 2nd ed.; Kluwer Academic: Boston, 1996.

methanol solution in 10 mL of methanol for 30 min under nitrogen at room temperature. A 30-mg sample of TOPO-coated nanocrystals was then added, producing a red, clear solution which was allowed to stir for an additional 24 h. To isolate the SNACs, the reaction mixture was reduced to 3 mL under vacuum and the SNACs were precipitated with 10 mL of acetone. The SNACs were further redissolved in 3 mL of methanol and precipitated again with 10 mL of acetone to ensure the removal of unreacted serotonin.

The concentration of SNAC solutions were determined by UV−visible spectroscopy using an extinction coefficient of 160 000 for a 30-Å nanocrystal (λ_{max}= 553 nm).[24] The extinction coefficient is arrived at by first determining the nanocrystal stoichiometry from Rutherford backscattering spectroscopy[25] and then determining the nanocrystal size and size distribution from transmission electron microscopy to arrive at a molecular weight for the nanocrystal. We determined the molecular weight of a 30-Å nanocrystal to be ∼68 500 including the TOPO ligands.[24]

Synthesis of the Serotonin-Linker Arm Ligand (1-[3-(2-Aminoethyl)-1*H*-indol-5-yloxy]-3,6-dioxa-8-mercaptooctane). 1-[3-(2-Aminoethyl)-1*H*-indol-5-yloxy]-3,6-dioxa-8-mercaptooctane (see Figure 3 for structure) was synthesized using an N-protected derivative of serotonin. This method used a generic linker arm containing a protected thiol and was coupled with the hydroxyl group of the N-protected derivative of serotonin. The protecting group was removed from the serotonin derivative followed by the protecting group on the thiol, resulting in 1-[3-(2-aminoethyl)-1*H*-indol-5-yloxy]-3,6-dioxa-8-mercaptooctane.

In this method, serotonin was protected using a phthalimido group to give a *N*,*N*-phthalimido-2-(5-hydroxy-1*H*-indole-3-yl)ethylamine. The generic linker arm consisted of a poly(ethylene glycol) derivative with a tosylate at one end and a *p*-methoxy benzyl thioether at the other end. We decided to synthesize the derivative based on the triethylene glycol as the starting materials were readily available from Aldrich.

The starting material for the linker arm was 2-[2-(2-chloroethoxy)-ethoxy]ethanol, and in the first step, the chlorine atom is replaced by refluxing 2-[2-(2-chloroethoxy)ethoxy]ethanol in ethanol over a period of 24 h under nitrogen with the sodium salt of *p*-methoxybenzylthiol. The nucleophilic displacement of chlorine results in 8-(4-methoxybenzylthio)-3,6-dioxaoctanol in a 71% yield. This is converted to a tosylate by stirring 8-(4-methoxybenzylthio)-3,6-dioxaoctanol in pyridine with an excess of tosyl chloride. This resulted in a 72% yield of 8-(4-methoxybenzylthio)-3,6-dioxaoctyl tosylate.

We coupled the *N*,*N*-phthalimido-2-(5-hydroxy-1*H*-indole-3-yl)-ethylamine to the linker arm by refluxing in acetone in the presence of 3 equiv of cesium carbonate for 18 h. This resulted in a 70% yield of 1-[3-[2-(*N*,*N*-phthalimido)ethyl]-1*H*-indol-5-yloxyl]-3,6-dioxa-8-(4-methoxybenzylthio)octane. The pthalimido functionality was removed from 1-[3-[2-(*N*,*N*-phthalimido)ethyl]-1*H*-indol-5-yloxyl]-3,6-dioxa-8-(4-methoxybenzylthio)octane by stirring for 2 h at room temperature in ethanol in the presence of excess hydrazine hydrate. This method gave a yield of 51% of 1-[3-(2-aminoethyl)-1*H*-indol-5-yloxyl]-3,6-dioxa-8-(4-methoxybenzylthio)octane.

Finally the *p*-methoxybenzyl protecting group on the sulfur atom was removed by stirring the 1-[3-(2-aminoethyl)-1*H*-indol-5-yloxyl]-3,6-dioxa-8-(4-methoxybenzylthio)octane in trifluoroacetic acid at 0 °C followed by treatment with hydrogen sulfide at room temperature in glacial acetic acid. This resulted in a yield of 39% of 1-[3-(2-aminoethyl)-1*H*-indol-5-yloxy]-3,6-dioxa-8-mercaptooctane.

Synthetic Materials and Methods. 2-[2-(2-chloroethoxy)ethoxy)]-ethanol, di-*tert*-butyl dicarbonate, and *N*-carbethoxyphthalimide were purchased from the Aldrich Chemical Co. 4-Methoxy-α-toluenethiol was purchased from Lancaster Synthesis. Serotonin creatine sulfate monohydrate was purchased from Fluka. Reagents were used as they were received. Thin-layer chromatography was carried out on precoated plates, and the products were visualized using UV light. Column chromatography on silica refers to silica gel obtained from Scientific Adsorbants Inc., Catalog No. 02826-25. NMR data were obtained using $CDCl_3$ as a solvent, and all NMR measurements were performed using a Brucker 300-MHz instrument. Chemical shifts were measured relative to TMS and coupling constants are measured in hertz. Low-resolution mass spectra (MS) were obtained from a Finigan Thermoquest TSQ 7000 triple quadrapole LC−MS equipped with an API-1 electrospray ionization source.

8-(4-Methoxybenzylthio)-3,6-dioxaoctanol. Sodium metal (0.8 g, 0.0348 mol) was added to ethanol (100 mL). After the sodium had completely reacted with the ethanol, 4-methoxy-α-toluenethiol (4.88 mL, 0.003 48 mol) was added.[26,27] The mixture was stirred at room temperature for 30 min and then 2-[2-(2-chloroethoxy)ethoxy]ethanol (5.88 g, 0.003 48 mol) was added. The reaction mixture was heated at reflux for 24 h. After being cooled to room temperature, it was poured into saturated ammonium chloride solution (40 mL) and extracted into dichloromethane (3 × 100 mL). The dichloromethane solution was dried over magnesium sulfate and upon evaporation yielded a yellow oil. The product was purified using column chromatography on silica eluted with a gradient system from dichloromethane to dichloromethane/methanol 10% to give 7.24 g (71%) of the product as yellow oil.

8-(4-Methoxybenzylthio)-3,6-dioxaoctyl Tosylate. 8-(4-Methoxybenzylthio)-3,6-dioxaoctanol (7.24 g, 0.025 mol) was added to dry pyridine (5 mL) and and the resultant mixture cooled to 0 °C under nitrogen. *p*-toluenesulfonyl chloride (6.5 g, 0.034 mol) was slowly added to this solution.[28] The mixture was allowed to warm to room temperature and was stirred for 18 h, after which it was added to water (100 mL) and dichloromethane (100 mL). The organic layer was separated and washed with hydrochloric acid (2 N, 1 × 50 mL) and sodium bicarbonate solution (saturated, 50 mL). Then it was dried over magnesium sulfate, and after filtration and evaporation, the crude product was obtained as a red oil. The product was purified using column chromatography in which the crude material had been adsorbed onto the silica and the column was eluted with a gradient system running from 20% diethyl ether/petroleum ether to 70% diethyl ether/petroleum ether. This gave 8.00 g (72%) of the product as a yellow oil.

1-[3-[2-(*N*,*N*-Phthalimido)ethyl]-1*H*-indol-5-yloxyl]-3,6-dioxa-8-(4-methoxybenzylthio)octane. 8-(4-Methoxybenzylthio)-3,6-dioxaoctyl tosylate (1.6 g, 0.0036 mol) was added to acetone (100 mL) and then *N*,*N*-phthalimido-2-(5-hydroxy-1*H*-indole-3-yl)ethylamine[29] (1 g, 0.0033 mol) was added. Dry cesium carbonate (3 g, 3 equiv) was added, and the mixture was heated at reflux for 24 h. The solution was cooled to room temperature and filtered. The product was purified using silica gel eluted with dichloromethane/98% methanol. This gave 1.1 g of 1-[3-[2-(*N*,*N*-phthalimido)ethyl]-1*H*-indol-5-yloxyl]-3,6-dioxa-8-(4-methoxybenzylthio)octane as a pale yellow oil.

1-[3-(2-Aminoethyl)-1*H*-indol-5-yloxyl]-3,6-dioxa-8-(4-methoxybenzylthio)octane. 1-[3-[2-(*N*,*N*-Phthalimido)ethyl]-1*H*-indol-5-yloxyl]-3,6-dioxa-8-(4-methoxybenzylthio)octane (1.4 g, 0.0024 mol) was dissolved in absolute ethanol (50 mL) and hydrazine monohydrate (2 mL). The solution was stirred for 18 h at room temperature and then evaporated. Dichloromethane (50 mL) was added to the resulting tar, and the mixture was heated at reflux for 30 min.[29] After cooling, it was filtered and evaporated and 1-[3-(2-aminoethyl)-1*H*-indol-5-yloxyl]-3,6-dioxa-8-(4-methoxybenzylthio)octane was purified using silica gel column chromatography eluted with dichloromethane 95%/triethylamine

(22) Murray, C. B.; Norris, D. J.; Bawendi, M. G. *J. Am. Chem. Soc.* **1993**, *115*, 8706−8715.
(23) Peng, X.; Wickham, J.; Alivisatos, A. P. *J. Am. Chem. Soc.* **1998**, *120*, 5343−5344.
(24) Folden, C. M. Honors Thesis, Vanderbilt University, 1999.
(25) Taylor, J.; Kippeny, T.; Rosenthal, S. J. *J. Cluster Sci.* In press.
(26) Boden, N.; Bushby, R.; Clarkson, S.; Evans, S.; Knowles, P.; Marsh, ?. ?. *Tetrahedron* **1997**, *31*, 10939−10951.
(27) Boden, N.; Bushby, R.; Liu, Q.; Evans, S.; Toby, A.; Jenkins, A.; Knowles, P.; Miles, R. *Tetrahedron* **1998**, *54*, 11537−11548.
(28) Almansa, C.; Mayo, A.; Serratosa, F. *Tetrahdron* **1991**, *47*, 5867−5876.
(29) Barf, T.; Boer, P.; Wikstrom, H.; Peroutka, S.; Svensson, K.; Ennis, M.; Ghazal, N.; McGuire, J.; Smith, M. *J. Med. Chem.* **1996**, *39*, 4717−4726.

3%/methanol 2%. This gave 0.6 g (51%) of 1-[3-(2-aminoethyl)-1*H*-indol-5-yloxyl]-3,6-dioxa-8-(4-methoxybenzylthio)octane as a pale yellow oil.

1-[3-(2-Aminoethyl)-1*H*-indol-5-yloxy]-3,6-dioxa-8-mercaptooctane. 1-[3-(2-Aminoethyl)-1*H*-indol-5-yloxyl]-3,6-dioxa-8-(4-methoxybenzylthio)octane (0.6 g, 0.0014 mol) was dissolved in trifluoroacetic acid (15 mL) and cooled to 0 °C. Anisole (1.5 mL) and mercury(II) acetate (0.516 g, 0.0016 mol) were added, and the mixture was stirred at 0° C for 2 h. The solution was evaporated, and the resulting solid was washed with diethyl ether (3 × 50 mL). After air-drying, the solid was dissolved in glacial acetic acid (25 mL) and hydrogen sulfide was bubbled through the solution for 30 min. Mercuric sulfide was removed by filtration, and the solution was evaporated to dryness.[30] The resulting oil was dissolved in dichloromethane and washed with sodium bicarbonate solution (1 M, 1 × 20 mL). The solution was dried over magnesium sulfate, filtered, and evaporated. This gave 0.2 g (39%) as a pale yellow oil: ^{1}H NMR ($CDCl_3$) δ 2.10 (br s, NH_2), 2.60 (t, J = 6.45 Hz, 2H), 2.78 (t, J = 6.84 Hz, 2H), 2.90 (t, J = 6.15 Hz, 2H), 3.42−3.66 (m, 6H), 3.82 (t, J = 5.13 Hz, 2H), 4.11 (t, J = 4.68 Hz, 2H), 6.74 (d, 1 ArH), 6.78 (d, 1 ArH), 6.89 (s, 1 ArH), 6.94 (d, 1 ArH), 7.15 (d, NH); *m*/*z* 324.39 [M^+], 325.09 [M^{1+}].

Synthesis of Core/Shell Nanocrystals and the Serotonin-Linker Arm−Nanocrystal Conjugates. TOPO-coated CdSe/ZnS core/shell nanocrystals (75-Å mean diameter) were synthesized according to the method of Dabbousi et al.[3] from 30-Å cores. TOPO-coated core/shells had a fluorescent quantum yield of 38%. To attach the serotonin ligand to the core/shells, the TOPO ligands were first exchanged with pyridine at 60 °C (60 mg of core/shells in 10 mL of pyridine, stir for 24 h). The serotonin ligands were dissolved in dicloromethane and added to the pyridine solution (60 °C). After 2 h, the nanocrystals were cooled to room temperature and precipitated with hexanes. As covering the entire surface of the nanocrystal with the serotonin ligand would introduce stearic interactions between the ligands and interfere with ligand−SERT interactions, we added mercaptoacetic acid, a short, water-soluble coligand, to the surface of the nanocrystal. The serotoin-linker arm-conjugated nanocrystals (LSNACs) were dissolved in equal volumes of DMF (1 mL) and mercaptoacetic acid (1 mL), and the resultant mixure was stirred for 24 h at room temperature. Two molar equivalents of potassium *tert*-butoxide was then added to this solution to neutralize the mercaptoacetic acid. The LSNACs were then collected by centrifugation, washed four times with methanol (20 mL), and dried under reduced pressure. The fluorescent quantum yield of the LSNCs drops to 3%.

HPLC Measurements. HPLC measurements were performed to ensure that free serotonin was not present in SNAC solutions or generated in cell assays. The analytical details for serotonin measurements were previously described by Lindsey.[31] The HPLC system consists of a Waters 501 pump, 712 WISP autosampler, 464 electrochemical detector, and Millennium 32 data system. The HPLC column used was a catecholamine column (3.9 × 100 mm) (Catalog No. C5100) from Chromosystems. The lower detection limit for serotonin was 2.5 nM.

Rutherford Backscattering Spectroscopy. Rutherford backscattering spectroscopy (RBS) was performed to estimate the extent of ligand coverage of the LSNACs. An iodinated derivative of the serotonin ligand was prepared such that iodine could be used as a marker in the RBS experiment. RBS on nanocrystals was previously described.[25] In this experiment, samples were prepared by dropping 0.2 mL of a concentrated iodinated LSNACs/pyridine solution onto a 1-cm^2 graphite substrate and wicking off excess solution. To obtain the I and Zn ratios, the individual peaks are integrated and normalized by the square of their atomic numbers.

Serotonin Transport Measurements. Human and *Drosophila* serotonin transporters (hSERT and dSERT, respectively) were transiently transfected into HeLa cells and grown at 37° in a 5% CO_2 humidified incubator. Cells were maintained in complete medium containing Dulbecco's minimal essential media (DMEM), 250 mg/L G418sulfate, 10% fetal bovine serum, 2 mM l-glutamine, 100 units/mL penicillin, and 100 μg/mL streptomycin and grown on poly(D-lysine)-coated 24-well plates. Cells were plated at a density of 100 000 cells/well and allowed to grow to a confluency for 2 days before assaying. The cells were assayed for tritiated serotonin transport in Krebs−Ringer−HEPES assay buffer as previously described.[32] Briefly, cells were washed in assay buffer (120 nM NaCl, 4.7 mM KCl, 2.2 mM $CaCl_2$, 1.2 mM $MgSO_4$ 1.2 mM KH_2PO_4 10 mM HEPES, pH 7.4), followed by a 10-min preincubation in 37 °C assay buffer containing 0.18% glucose. Cells were incubated in assay buffer for 10 min at 37 °C with varying concentrations of unconjugated or conjugated nanocrystals with 20 nM tritiated serotonin (110 C_i/mmol), 100 μM pargyline, and 100 μM ascorbic acid. Assays were terminated by washing three times with ice-cold assay buffer. The cells were dissolved in OptiPhase scintillation fluid, and accumulated tritiated serotonin was quantified by liquid scintillation counting using a Wallac Microbeta plate reader. Specific uptake was determined by subtracting data from experiments in which cells were treated with 0.5 μM paroxetine, a high-affinity SERT antagonist. The estimated half-maximal (EC_{50}) values were derived using a nonlinear least-squares curve fit (Kaleidagraph, Synergy Software). Experiments were performed in duplicate or triplicate and repeated in two or more separate assays. Means were compared using a two-sided Student *t*-test (Graph-Pad InStat for MacIntosh).

Electrophysiology Measurements. *Xenopus* Oocyte Electrophysiology. Plasmids (pBluescript-SKII) containing the human serotonin receptor $5HT_3$ or hSERT cDNA were linearized with *Not*I and transcribed with the mMessage Machine T7 In Vitro Transcription Kit (Ambion, Austin, TX). The hSERT coding region is flanked 5′ by alfalfa mosaic virus and 3′ by *Xenopus* β-globin UTRs. Stage V and VI oocytes were harvested, defolliculated, and injected with 40 ng of $5HT_3$ or 24 ng of hSERT cRNA.[33−35] The oocytes were maintained at 18 °C for 18 days, in Ringer's media (in mM: 96 NaCl, 2 KCl, 5 $MgCl_2$, 5 Hepes; pH 7.6) supplemented with 0.6 mM $CaCl_2$, 5% dialyzed horse serum (GIBCO−BRL/ Life Technology), 50 μg/mL tetracycline, 100 μg/mL streptomycin, and 550 μg/mL sodium pyruvate.

Electrophysiologoical experiments were performed in the modified cut-open oocyte voltage clamp configuration.[36] A key element of this technique is that ~10% of the total oocyte surface is electrically isolated, so that the transmembrane potential can be controlled, while both faces of the membrane are also accessible for treatment with experimental solutions. The apparatus was purchased from Dagan Corp. (Minneapolis, MN), and voltage protocols were applied with a Dagan CA-1B amplifier. Data were digitized with a DigiData 1200 Interface (Axon Instruments, Foster City, CA) and collected by a PC running pClamp v. 7.0 software (Axon Instruments). The external membrane of the oocyte was superfused at ~1 mL/min with Ringer's media containing 100 μM $CaCl_2$, 100 μM pargyline, 100 μM ascorbic acid, 200 μM niflumic acid, and the concentration of serotonin or LSNAC indicated. The internal face of the oocyte was perfused at 20−80 μL/min with internal oocyte solution (in mM: 50 KCl, 5 NaCl, 50 KOH, 70 methanesulfonic acid, 10 Hepes, 2 $MgCl_2$, 0.1 EGTA; pH 7.4). $CaCl_2$ was added such that the final free Ca concentration was 50 nM. Oocytes were first clamped to −60 mV until a stable baseline was achieved, ~10 min. For $5HT_3$, the external serotonin or LSNAC perfusion was then begun, holding the voltage clamped and acquiring data at 10 Hz.

(30) Gordon, E.; Godfrey, J.; Delaney, N.; Asaad, M.; Von Langen, D.; Cushman, D. *J. Med. Chem.* **1988**, *31*, 2199−2211.
(31) Lindsey, J. W. *J. Toxicol. Environ. Health A* **1998**, *54*, 421−429
(32) Barker, E. L.; Perlman, M. A.; Adkins, E. M.; Houlihan, W. J.; Pristupa, Z. B.; Niznik, H. B.; Blakely, R. D. *J. Biol. Chem.* **1998**, *273*, 19459−19468.
(33) Goldin, A.L. *Methods Enzymol.* **1992**, *207*, 266−279.
(34) Stuhmer, W. *Methods Enzymol.* **1998**, *293*, 280−300.
(35) Elsner, H.-A.; Honck, H.-H.; Willmann, F.; Kreienkamp H.-J.; Iglauer, F. *Comp. Med.* **2000**, *50*, 206−211.
(36) Costa, A. C. S.; Patrick, J. W.; Dani, J. A. *Biophys. J.* **1994**, *67*, 395−401.

For hSERT, serotonin or LSNAC was perfused onto the oocyte and a voltage ramp from −120 to +80 mV lasting 640 ms was applied to the oocyte until the drug-induced current stabilized. hSERT data were filtered at 2 kHz and digitized at 10 kHz. No serotonin-induced currents were observed in oocytes that had not been injected with cRNA.

Microscopy. Imaging studies were performed using HEK-293 cells stably transfected with hSERT.[13] Transfected HEK-293 cells and the parental HEK-293 cells were plated on polylysine-coated coverslips in 24-well plates and grown to 80% confluency. The cells were maintained at 37 °C throughout all steps until visualization. Transfected and parental cells were preincubated in blocking solution [5% normal goat serum (NGS) (Jackson Immunoresearch)/0.1% cold water fish skin gelatin (Amersham)/Krebs−Ringer−HEPES buffer (KRH)] for 5 min, rinsed with pure KRH, exposed to a solution of SNACs in blocking solution for 5 min, and rinsed with KRH. To demonstrate the specificity of binding by SNACs, parental and transfected cells were exposed to an inhibitor cocktail containing the specific SERT inhibitor paroxetine (30 μM), the monoamineoxidase inhibitor pargyline (10 μM), and an antioxidant, ascorbic acid (10 μM) in blocking solution for 5 and 10 min, respectively. The cells were then rinsed with 1% NGS/KRH, exposed to a solution of SNACs in the inhibitor/blocking solution for 5 min, and washed once with 1% NGS/KRH. SNAC excitation was achieved with a mercury excitation source. Images were collected with a TRITC filter set. Images were captured with an Optronics three-chip color camera (700-line resolution) on a Zeiss Axioplan microscope.

Results and Discussion

The preparation of SNACs is outlined in Figure 1. The amine functionality of serotonin is protonated at physiological pH.[37] Since a protonated amine is necessary for recognition at the serotonin transporter,[37] we developed a strategy to attach the serotonin to the nanocrystal through the 5′-hydroxyl functionality. The tetramethylammonium hydroxide serves to remove the phenolic proton of serotonin, allowing the electronegative oxygen atom to covalently bond to surface Cd atoms on the nanocrystals, displacing the trioctylphosphine oxide capping ligands. We verified that if serotonin was not added to the tetramethylammonium hydroxide/methanol solution prior to the addition of the trioctylphosphine oxide-coated nanocrystals the nanocrystals are insoluble, indicating good displacement of the trioctylphosphine oxide ligands by the deprotonated serotonin ligand. The exact surface coverage of serotonin was not determined; however, if every trioctylphosphine oxide ligand is replaced with serotonin, the surface coverage would be 70%, corresponding to ∼200 serotonin molecules.[25] The SNACs are partially soluble in water, completely soluble in dimethyl sulfoxide, and insoluble in toluene, further indicating good displacement of serotonin for trioctylphosphine oxide. To determine the concentration at which SNACs effectively block the uptake of serotonin by the serotonin transporter, it is necessary to first be able to determine the concentration of SNACs in solution. This was determined using the gram molecular weight of trioctylphosphine oxide-coated nanocrystals as determined by stoichiometry measurements obtained from Rutherford backscattering data[25] and assuming 1 for 1 exchange of serotonin for the trioctylphosphine oxide. We estimate the upper uncertainty in SNAC concentration to be 15%.

Figure 2A displays the results of inhibition studies with SNACS for tritiated serotonin uptake using hSERT and dSERT as well as parallel competition studies using unconjugated serotonin (dashed line). An estimate of SNAC EC_{50} values, the concentration at which half of the serotonin uptake is inhibited, was determined by nonlinear regression. We obtained an EC_{50} value of 99 μM for hSERT and 33 μM for dSERT. The slope of the inhibition curve yields a Hill coefficient estimate of 1.0, consistent with interaction at a single binding site. The serotonin uptake measured was SERT-dependent as uptake was inhibited by the serotonin selective reuptake inhibitor paroxetine. By comparing the SNAC inhibition of tritiated serotonin transport with that achieved by unlabeled serotonin, we see the SNACs are 1−2 orders of magnitude less potent than free serotonin. This difference most likely originates from the steric bulk of the nanocrystal. The decrease could also originate from incomplete substitution of serotonin for trioctylphosphine oxide.

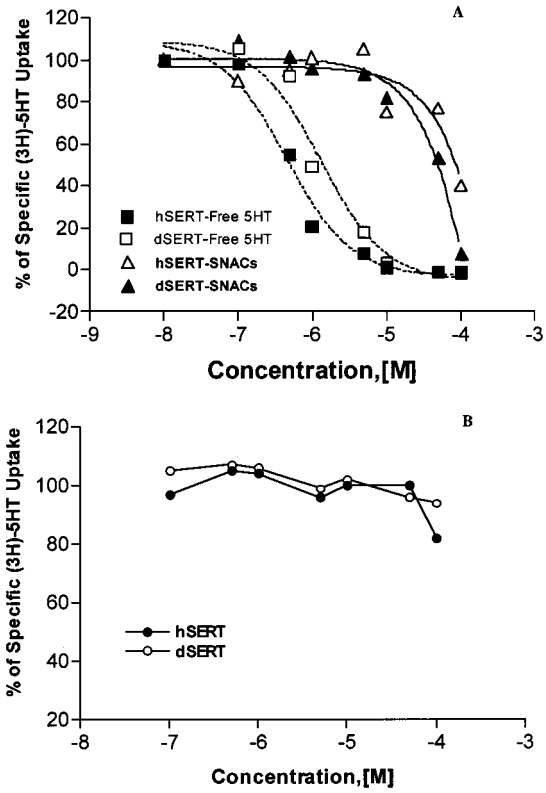

Figure 2. (A) Tritiated serotonin transport inhibition assays comparing free, unlabeled serotonin and SNACs at *Drosophila* and human SERT proteins (dSERT and hSERT, respectively). EC_{50} values ± standard error for inhibition are dSERT/ 5HT, 1.2 ± 0.3 μM; SNACs, 33.1 ± 13.3 μM/ hSERT/5HT, 0.42 ± 0.13 μM; SNACs, 99.2 ± 14.1 μM. Fits and errors are derived from three replicate inhibition assays performed in triplicate on transfected HELA cells. (B) Lack of inhibition of hSERT or dSERT by unconjugated, mercaptoacetic acid-coated nanocrystals. Serotonin uptake assays for SNACs and free serotonin by hSERT, and dSERT.

We used HPLC to evaluate whether traces of free serotonin remain after SNAC preparation or whether leaching of serotonin off the nanocrystals occurs and it is inadvertently introduced to the tritiated-serotonin uptake assay. At a SNAC concentration of 50 μM, free serotonin would need to reach a concentration of ∼500 nM to account for the observed SNAC inhibition of tritiated serotonin uptake. In the HPLC test, SNACs at a concentration of 100 μM were incubated in conditions that mimicked the uptake assay; i.e., SNACs were placed in buffer solution with stably transfected hSERT and dSERT HEK 293 cells. After 10 min, the SNAC-containing buffer was removed and analyzed for free serotonin by HPLC. No free serotonin could be detected (lower detection limit 2.5 nM), indicating that serotonin in not appreciably liberated during the uptake assay.

(37) Keyes, S.; Rudnick, G. *J. Biol. Chem. 257*, 1172−1176.

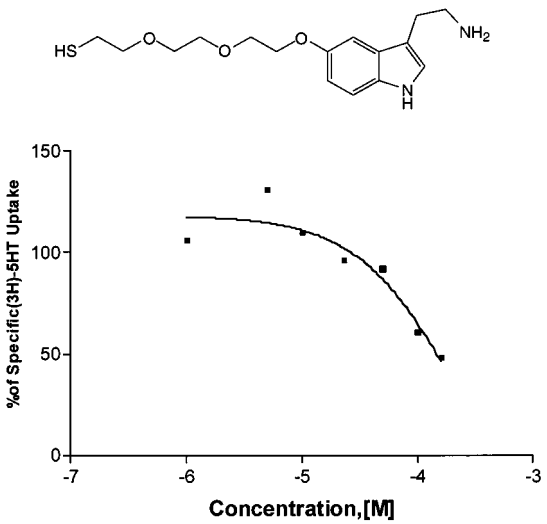

Figure 3. Tritiated serotonin transport inhibition assay with LSNACs at hSERT. Inset: Altered serotonin ligand. The thiol terminus allows for covalent attachment to Zn on the surface of the core/shell nanocrystal. The water-soluble, flexible spacer provides distance between the nanocrystal and the serotonin to reduce the probability of nanocrystal-to-ligand charge transfer and allow additional degrees of freedom to the ligand. Estimated EC_{50} for inhibition, 115 ± 12.5 μM.

To further confirm that serotonin does not leach off the nanocrystals, a solution of SNACs was dialyzed against 1 L of buffer overnight and uptake inhibition assays were repeated. The dialyzed SNACs displayed the same potency for the transporters as SNACs that had not been dialyzed, again suggesting that serotonin bound to the nanocrystal gives rise to the biological activity of the SNACs.

Finally, to validate specificity of SNACs inhibition of serotonin transport, we performed an uptake assay using nanocrystals coated only with mercaptoacetic acid. Results from these studies are displayed in Figure 2B. We find there is no inhibition of SERT by mercaptoacetic acid-conjugated nanocrystals over the same concentration range tested for SNACs, indicating that serotonin modification of nanocrystals is needed to affect inhibition of transport activity.

When serotonin is directly attached to fluorescent CdSe/ZnS core/shell nanocrystals according to the method described above, the fluorescence is quenched, presumably through charge-transfer interactions with the serotonin ligand. Attaching serotonin to the core/shell nanocrystals through a linker arm helps both to defeat charge transfer and to give the ligand additional degrees of freedom for interactions with SERT. We synthesized the ligand shown in Figure 3 and attached it to CdSe/ZnS core/shell nanocrystals via ligand exchange. The ligand is designed with a thiol anchor and a flexible, water-soluble spacer. A mercaptoacetic acid cosolubility ligand is added to aid in water solubility.

The results of inhibition studies with LSNACs for tritiated serotonin uptake using hSERT is displayed in Figure 3. From these data we obtain an EC_{50} value of 115 μM, which is quite similar to the value obtained when serotonin is conjugated directly to the nanocrystal (99 μM). While serotonin on the LSNACs has the benefit of being displaced from the steric bulk of the nanocrystal by the linker arm when compared to the SNACs, the oxygen atoms of the linker arm may be involved in unfavorable hydrogen bonding, which limits the activity of the ligand. In a separate study, we assayed a selective ligand for the dopamine transporter that has the same polyether linker arm and found an EC_{50} value of 5 μm. When the linker arm was replaced with an alkyl chain of the same length, the activity increased to 17 nm, implicating unfavorable hydrogen-bonding interactions with the polyether chain.[38]

To quantify the extent of ligand coverage on the LSNACs, we devised a strategy to determine the effectiveness of the ligand coupling reaction using Rutherford backscattering spectroscopy.

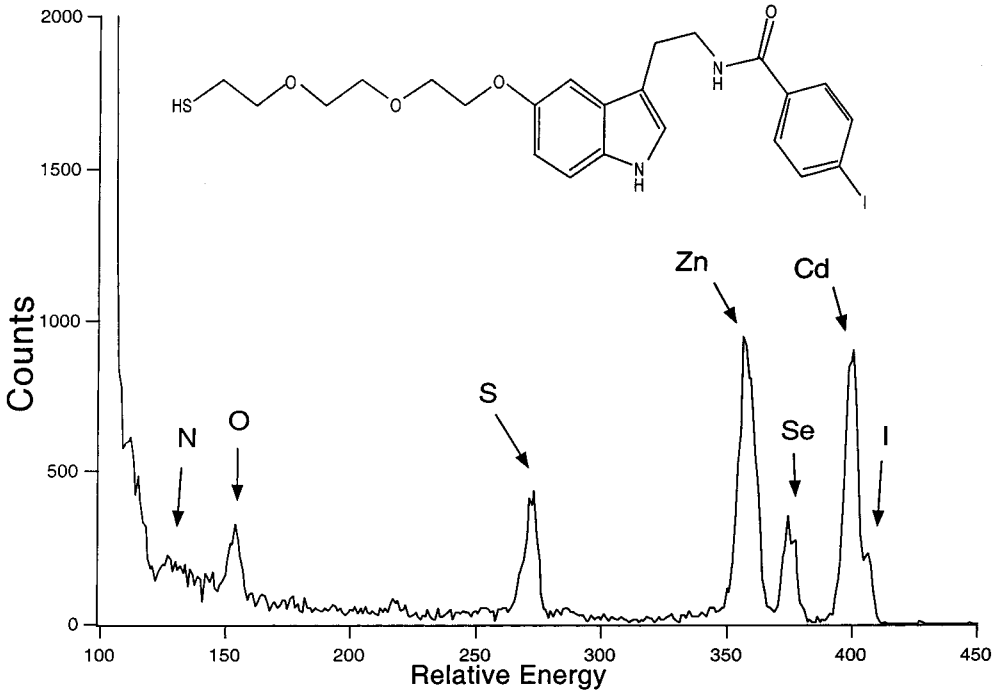

Figure 4. Iodinated serotonin ligand and Rutherford backscattering spectrum of iodinated serotonin-conjugated core/shells. Peaks for individual elements are indicated. The ratio of the Zn-to-Cd peaks is consistent with a 15-Å shell surrounding a 20-Å core. The I/Zn ratio is used to determine the ligand coverage and consequently the efficiency of the coupling reaction.

We synthesized an iodinated derivative of the serotonin ligand (Figure 4) that has steric bulk similar to that of the serotonin ligand and should thus give the same coverage. The iodine atom serves as a marker by which to count individual ligands on the surface of the nanocrystals. The RBS spectrum (Figure 4) clearly indicates the Cd and Se peaks corresponding to the core nanocrystal and the Zn and S peaks of the shell, as well as the I of the ligand. The intensity of the peaks is proportional to the square of the atomic number of the element and its relative abundance. These core shells were the same as used in the inhibition studies and had a 20-Å core with a 15-Å shell. To obtain the percentage ligand coverage from the Zn/I ratio, the core/shells are assumed to be spherical. Since the molar equivalents of core/shells and iodinated ligands used in the coupling reaction are known, the efficiency of the ligand coupling reaction can be determined. The iodonated ligands are not displaced from the nanocrystal when the mercaptoacetic acid cosolubility ligand is added, as was verified by RBS. From this analysis, the efficiency of the coupling reaction is determined to be 80%. Using this coupling efficiency, we estimate the LSNACs used in the inhibition studies had ~160 serotonin ligands/nanocrystal.

To further investigate LSNAC−receptor interactions, we measured the electrophysiologicol response of the serotonin-3 receptor ($5HT_3$) and the transporter when exposed to LSNACs. Figure 5A shows currents elicited from an oocyte expressing the ionotropic $5HT_3$ receptor, when exposed to either various concentrations of serotonin or 1 μM LSNAC with the transmembrane potential clamped at −60 mV. Free serotonin induces large, inactivating inward currents in oocytes expressing the ionotropic $5HT_3$ receptor, at −60 mV. This current increases dramatically with serotonin concentration due to cooperative binding of serotonin at the receptor. We measured response of the receptor to varying serotonin concentations in similarly treated oocytes (data not shown; three oocytes) and fit the results to the Hill equation $I/I_{max} = [\text{serotonin}]^n/(EC_{50}{}^n + [\text{serotonin}]^n)$, with $n = 2.17 \pm 0.08$ and $EC_{50} = 1.67 \pm 0.04$ μM.

Exposure to 1 μM LSNAC failed to elicit a current from the $5HT_3$ receptor (Figure 5A and inset). On the basis of the data recorded, we would have detected any current larger than ~5 nA, activated for at least 0.5 s. One possibility is that LSNACs do not reach the binding site of the $5HT_3$ receptor. Structural studies of the $5HT_3$ receptor and the closely related nicotinic acetylcholine receptor indicate that the binding site is located in a small niche on the side of a 2−3-nm pore.[39,40] Thus, the nanocrystal may prevent the seotonin ligand from reaching its binding site. It is also possible, however, that the nanocrystal-bound serotonin does reach its binding site but fails to gate the channel, due to the presence of the nanocrystal. Finally, it is possible that the channel gates properly, but the pore is blocked by the nanocrystal. Further experiments are necessary to distinguish these possibilities.

Examination of Figure 5A also allows us to put a limit on the concentration of free serotonin accompanying the LSNACs, if we assume that in fact the LSNACs do not elicit a current through the receptor because they do not reach the binding site at all. In this case, using our measured Hill coefficient (n) and EC_{50}, the Hill equation indicates that, for a response of less than 5 nA, there could be no more than ~50 nM free serotonin in the solution containing 1μM LSNAC.

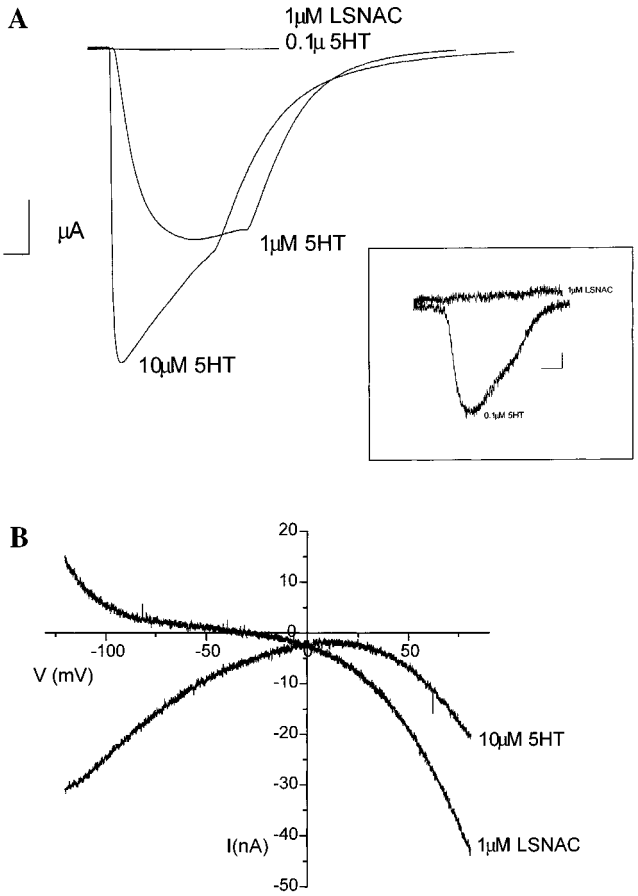

Figure 5. Electrophysiological currents elicited by serotonin or LSNACs. (A) Currents recorded from the serotonin receptor 5HT3 with the membrane potential clamped to −60 mV. Application of 10, 1, or 0.1 μM free serotonin results in measurable current through the receptor, but application of 1 μM LSNAC does not. Inset: Expanded view of the 0.1 μM serotonin and LSNAC recording. (B) Currents recorded from hSERT as a function of linearly changing membrane potential V. The current induced by serotonin is typical. The current induced by LSNACs is characteristic of currents induced by hSERT antagonists.

Figure 5B shows the currents elicited from an hSERT expressing oocyte, exposed to either 10 μM serotonin or 1 μM LSNAC, and subjected to a voltage ramp from −120 to +80 mV. Currents are expressed as the difference between the current measured in the presence and absence of serotonin or LSNAC. Thus, serotonin-insensitive background currents in the oocyte are subtracted out, so that the displayed current represents the current through hSERT alone.

The serotonin-induced current is typical of currents observed previously from SERT;[41] in particular, note that it remains negative over the tested potential range. Thus, hSERT is functioning in the expected manner under these experimental conditions.

Exposure to 1 μM LSNAC elicited a current that differs qualitatively from the serotonin-induced current, reversing near −30 mV. This current closely resembles reported currents

(38) Tomlinson, I.; Blakely, R. D.; Rosenthal, S. J., unpublished.
(39) Boess, F.G.; Beroukhim, R.; Martin, I. L. *J. Neurochem.* **1995**, *64*, 1401−1405.
(40) Miyazawa, A..; Fujiyoshi, Y.; Stowell, M.; Unwin, N. *J. Mol. Biol.* **1999**, *288*, 765−768.
(41) Mager, S.; Min, X.; Henry, D. J.; Chavkin, C.; Hoffman, B. J.; Davidson, N.; Lester, H. A. *Neuron* **1994**, *12*, 845−859.

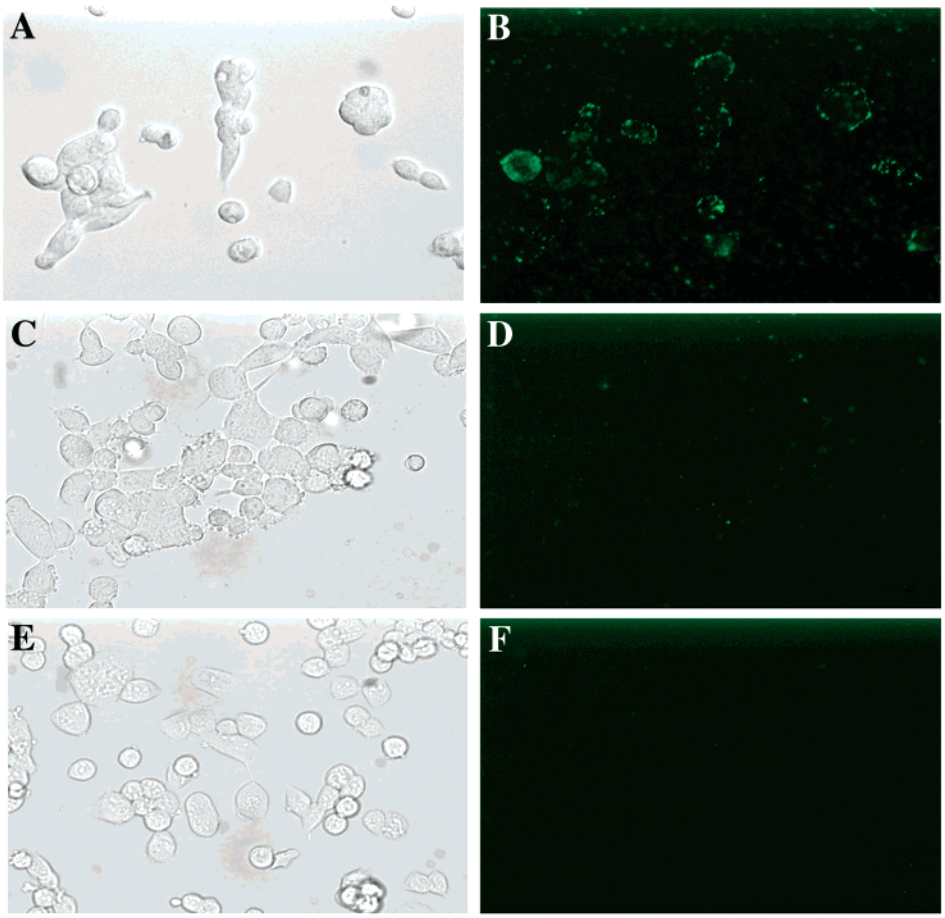

Figure 6. Left: differential interference contrast images. Right: identical field of view; fluorescence images. Top: HEK cells with hSERTs in the cell membrane. Fluorescence labeling of the hSERTs in the membrane is clearly visible. Center: HEK cells that do not have hSERT in the cell membrane. No fluorescence labeling is visible. Right: HEK cells with hSERT in the membrane. These cells were exposed to an antagonist before being exposed to LSNACs. No fluorescence labeling is visible.

elicited by nontransported antagonists of hSERT such as the serotonin-selective reuptake inhibitors fluoxetine (Prozac) or paroxetine (Paxil).[41] These antagonist-induced currents are due to the blockage of a constitutive leak current through hSERT (the current that slips through the transporter in the absence of serotonin), rather than the activation of a current. Thus, the observed current in the presence of LSNAC indicates that LSNACs interact with hSERT, block the permeation pathway of a constitutive leak current, and are not transported. We presume that LSNACs are binding to a site at least overlapping the antagonist binding site and most likely the serotonin-binding site.

To directly validate LSNACs interactions, we tested whether we could visualize SERT protein expression on the surface of HEK cells. Data from these studies are presented in Figure 6. Panels on the left in Figure 6 display cells as viewed using standard brightfield illumination, while panels on the right are the identical fields imaged under fluorescence. Cells in the top panels have been transfected with hSERT, and fluorescence labeling of hSERT by the LSNACs is clearly visible. Labeling appears punctate and circumferential with far less labeling of the acellular matrix onto which the cells are plated. The center panels display results with nontransfected HEK-293 cells. No visible nonspecific binding of LSNACs was evident. The bottom panels display results with HEK-hSERT cells where LSNACs incubation included the high-affinity hSERT antagonist, paroxetine (30 μM), before being exposed to the fluorescent LSNACs. Paroxetine coincubation completely eliminated surface labeling of HEK-hSERT cells by LSNACs, further documenting the specificity of SNAC−SERT interactions.

Our ability to visualize transfected cells with serotonin-conjugated nanocrystals suggests that the nanoconjugates have a reasonably high affinity for SERT proteins despite the relatively low potency exhibited in transport inhibition assays. One explanation for this discrepancy may be that the free nanocrystals available for transporter interaction may be overestimated. We calculate the concentrations of our nanocrystals using UV−visible spectroscopy, and this may overestimate the number of nanocrystals with productive coupling. In addition, an unknown proportion of nanocrystals may be inaccessible to the transporter due to aggregation or other nonspecific associations. Finally, the multivalent nature of the conjugated nanocrystals may limit dissociation to such an extent that measures of potency report only fractional occupancy rather than competitive kinetics against the transporter's substrate 5-HT. Further studies are needed to directly assess the intrinsic rate constants for target association and dissociation.

Several of the fluorescence labeling experiments we performed were contaminated by varying degrees with nonspecific binding on the parental cells. We believe this to be due to residual TOPO or a strongly binding impurity in the TOPO which is not removed from the surface of the core/shells during

the pyridine exchange. Incomplete removal of TOPO after pyridine exchange has been verified by XPS spectroscopy.[42] Residual TOPO on the core/shells would lead to nonspecific binding as the octyl chains would be lipophilic. Recently Bruchez et al. prepared core/shell surfaces presenting poly(ethylene glycol) which substantially reduced nonspecific binding.[43] In future applications, we plan to covalently link our ligands to these core/shells, thereby eliminating problems with nonspecific binding.

Conclusions

We prepared serotonin-labeled nanocrystals and demonstrated that serotonin-labeled nanocrystals inhibit serotonin transport activity in transfected cells. Electrophysiology measurements indicate that serotonin-conjugated nanocrystals do not elicit currents when exposed to the $5HT_3$ receptor but they do elicit currents when exposed to the transporter which are similar to those induced by antagonists. We also prepared fluorescent serotonin-labeled nanocrystals and demonstrated that they can be used to visualize SERTs on the plasma membrane of HEK cells. These probes can assist in determining the structure of SERT and transporter regulation. One drawback at present is the relatively weak potency of SNACs relative to typical high-affinity antagonists and antibodies used for autoradiography and immunocytochemistry. Moreover, the current formulation cannot discriminate serotonin transporters from serotonin receptors when these proteins coexist, as in neural tissue. Future studies will focus on improving ligand-conjugated nanocrystal potency and specificity through attachment of well-characterized, high-affinity transporter and receptor antagonists. Additional studies are also needed to evaluate further the structural determinants of SERT−nanocrystal interactions and the degree to which nanocrystal technology can be implemented to identify and study specific proteins in living cells. Regardless, these findings support further consideration of ligand-conjugated nanocrystals as versatile probes of membrane proteins in living cells.

Acknowledgment. We gratefully acknowledge Ray Johnson in the Center for Molecular Neuroscience Core for performing the HPLC measurements and Qiao Han for assistance with uptake measurements. We are also indebted to Fred Mikulec for several helpful discussions concerning core/shell synthesis, and we are grateful to Quantum Dot Corp. for helpful discussions and providing some of the core/shells used in this study. We acknowledge Hongping Yuan for oocyte and RNA preparations. Finally, we acknowledge access to the Ion Scattering Facility at Vanderbilt University. This work was supported by a Discovery Grant from Vanderbilt University Central (S.J.R., I.T.), a Pilot Grant from the Vanderbilt University Medical Center (R.D.B., S.S.), PHS Grant 5RO3MH61874-02 (S.J.R., I.T.), PHS Grant DA07390 (R.D.B.), NIH NS-34075 (L.J.D., S.V.A.), and NRSA MH12399 (E.M.A.).

JA003486S

(42) Bowen Katari, J. E.; Colvin, V. L.; Alivisatos, A. P. *J. Phys. Chem*, **1994**, 98, 4109−4117.
(43) Bruchez, M, private communication.